Histomorphometric analysis of the proximal portion of the femur in healthy dogs

David T. Edinger, DVM; Kei Hayashi, DVM, PhD; Yao Hongyu, MS; Mark D. Markel, DVM, PhD; Paul A. Manley, DVM, MSc

Objective—To describe the cancellous bone architecture of the head and neck of the femur in healthy dogs by use of automated histomorphometry techniques in conjunction with histologic grading of articular cartilage.

Animals—30 mature male dogs with healthy coxofemoral joints

Procedure—Dogs were 1.5 to 4 years old and weighed 27 to 37 kg. Computer images of fine-detail radiographs of 100-µm-thick coronal and transverse plane sections of the head and neck of the femur (14 dogs) were analyzed by use of histomorphometry software. Statistical comparisons among histomorphometric indices of 4 regions were performed. Histologic preparations of coronal and transverse plane sections of femoral head articular cartilage (16 dogs) were graded. Median grades for lateral, medial, cranial, and caudal halves of the femoral head articular cartilage were determined.

Results—Bone volume/total volume, trabecular thickness and number, and bone surface/total volume were significantly higher in the femoral head than in the femoral neck. Anisotropy (trabecular alignment) and trabecular separation were significantly higher in the femoral neck than in the femoral head. Anisotropy was significantly higher in the caudal half of the femoral neck than in the cranial half. Cartilage had histologic grades indicating health without significant differences among lateral, medial, cranial, and caudal halves of femoral head cartilage.

Conclusions and Clinical Relevance—A predictable cancellous architecture in the head and neck of the femur is associated with healthy cartilage. (*Am J Vet Res* 2000;61:268–274)

The cancellous architecture of the proximal portion of the femur in humans was described by Meyer[1] and later by Wolff[2] as consisting of struts of bone arranged in trajectories that resist applied forces. Subsequently, several authors have diagrammed the trabecular arrangement in 2[3-5] and 3[6,7] dimensions. Cancellous bone has been described as a material optimally designed to prevent fracture and collapse, with minimal bulk.[8,9]

In the proximal portion of the femur in humans, there are groupings of trabeculae referred to as primary and secondary compressive groups and primary and secondary tensile groups.[5] The primary compressive group is located on the medial side of the femoral neck, continuing to the superior aspect of the femoral head. The primary tensile group is located on the lateral side of the femoral neck, arcing medially to the inferior aspect of the femoral head. Elke et al[7] used standard computed tomography on stripped, mature human cadaver femurs and, in contrast to Singh et al,[5] found a sharp distinction in trabecular architecture between the epiphysis and metaphysis. The cancellous bone of the epiphysis had a random or isotropic pattern. The cancellous bone of the metaphysis had distinctly aligned, anisotropic patterns. The physeal scar represented a distinct bony division between the epiphysis and metaphysis, and the bundles of trabeculae from the metaphysis were redirected on the epiphyseal side of the scar.[7] A change in bone pattern at the physeal scar in the proximal region of the femur in mature humans has been reported.[3,6]

Histomorphometric analysis of the proximal portion of the femur in dogs, to our knowledge, has not been reported, but results of 1 study suggested that the trabeculae in the proximal portion of the femur were aligned and not randomly arranged.[10] Vahey et al[10] found that the cancellous bone of the femoral head and neck in dogs had "anisotropic behavior," on the basis of mean stiffness measurements recorded from cubes of cancellous bone from 2 canine femurs that were normal in appearance. The cubes were compressed in the proximal to distal, medial to lateral, and cranial to caudal directions, and had greater mean stiffness in the proximal to distal direction. No attempt was made to quantify the degree of organization (the anisotropy), but the authors suggested that orientation of trabeculae parallel to the proximal-distal axis was responsible for the greater stiffness.[10]

Radin et al[11,12] suggested that the health of articular cartilage was dependent on the mechanical qualities of the underlying bone. Cartilage changes in rabbit knees were preceded by stiffening of the proximal tibial cancellous bone.[13] Damaged areas of femoral condylar articular cartilage in sheep were associated with a reorientation (increased anisotropy) of distal femoral trabeculae towards the femoral-tibial articulation.[14] The spatial arrangement of trabeculae in humans was significantly changed in the distal portion of the femur in areas of stiffened subchondral bone associated with loss of cartilage mucopolysaccharide.[15] We presumed that the architecture of canine cancellous bone could also change in association with osteoarthritis.

Results of several studies indicate that the anisotropic arrangement of trabeculae plays a major role in mechanical stiffness.[16-18] A finite element model revealed that stiffness measured at the subchondral plate varied depending on the arrangement of underlying trabeculae. Variations in the arrangement of trabeculae underlying cartilage implied nonuniform compression

Received Dec 11, 1998.
Accepted May 18, 1999.
From the Comparative Orthopaedic Research Laboratory, Departments of Departmetns of Surgical (Edinger, Manley) and Medical (Hayashi, Markel) Sciences, and Materials Science and Engineering (Hongyu) University of Wisconsin, Madison, WI, 53706. Dr. Edinger's present address is 309 N Rosa Rd, Madison, WI 53705.
The authors thank Dr. R. O'Brien, J. Wingren, and W. Thal for technical assistance, and Dr. R. Peterson for the illustrations.

of the cartilage under load, which may play a role in joint degeneration.[19] Documenting trabecular indices and trabecular arrangement of the proximal portion of the femur in healthy, mature dogs would aid subsequent studies that attempt to relate changes in the underlying cancellous bone to changes in the articular cartilage.

We hypothesized that there is a consistent and quantifiable microarchitecture in the proximal portion of the femur in healthy (nonarthritic) dogs. Cartilage grading based on an accepted histologic grading system[20] would support the model as normal/nonarthritic. The objective of the study reported here was to describe the cancellous bone architecture of the proximal portion of the femur in healthy mature dogs by use of automated histomorphometry techniques in conjunction with histologic grading of articular cartilage.

Materials and Methods

Bone specimen preparation—The proximal portion of the femur (n = 16) was obtained from 14 mature, sexually intact male dogs from an unrelated study; dogs were 1.5 to 4 years old and weighed from 27 to 37 kg. All dogs were research-based mixed-breed hounds housed on concrete flooring. The coxofemoral joints had no evidence of osteoarthritic change on standard pelvic radiographs. The articular cartilage was grossly normal in appearance.

Eight specimens were sectioned in a coronal plane, and 8 were sectioned transversely, using a precision saw with a diamond wafering blade.[a] Three equally spaced sections were obtained in each plane from each specimen (**Fig 1 and 2**). Each of 48 sections was embedded in polymethylmethacrylate,[b] cut to 200 to 300 µm thickness, and ground to 100 µm by use of a speed lapping machine.[c] High-detailed radiography was performed on each 100-µm section with high-resolution radiographic film[d] within a cabinet radiographic unit.[e]

Histomorphometry—Images of microradiographs were obtained by scanning[f] at 150 dots/in to a magnification of 15X on a personal computer.[g] The achieved resolution of each image was 11.3 µm/pixel. All images were stored by use of an image processing program.[h] Each image was rotated so that all were of the same orientation; the articular surface faced the bottom edge of the screen, and the femoral neck extended to the top of the screen. The medial aspect of the image was oriented to the viewer's left for coronal sections, and the cranial aspect of the image was oriented to the viewer's left for transverse sections (**Fig 3**); this resulted in consistent region identification for coronal and transverse sections. Two of the 48 computer images had a grey appearance instead of the typical strongly contrasting black and white appearance; the 2 microradiographs scanned to create these images were reexamined and found to lack the black and white contrast of the other microradiographs. These 2 computer images were not used for analysis.

Custom software (developed on the basis of a widely used directed secant algorithm[16,21,22]) was used for histomorphometric analysis. A threshold value was selected that calibrated the software to correctly identify a pixel as either white (bone) or black (marrow space). To choose the threshold, an area from each of 4 randomly selected computer images was located on the microradiograph and hand-digitized from the

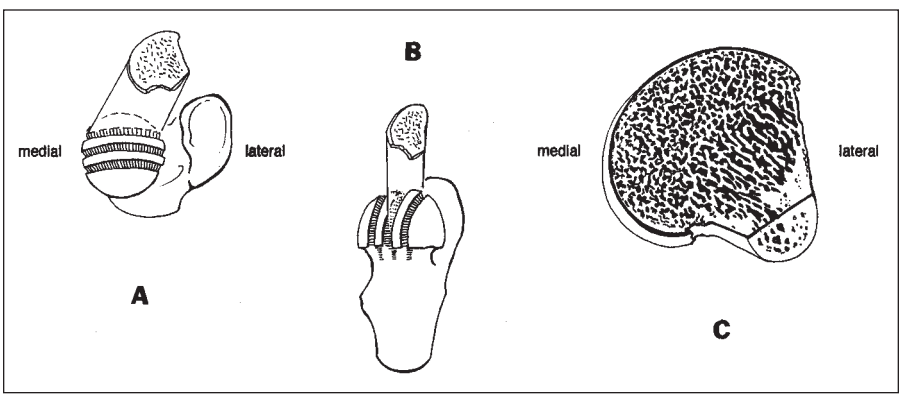

Figure 1—Illustration of coronal sectioning of the femoral head of a healthy dog. A—Proximal to distal view. B—Medial to lateral view. C—Cranial to caudal view of cancellous architecture.

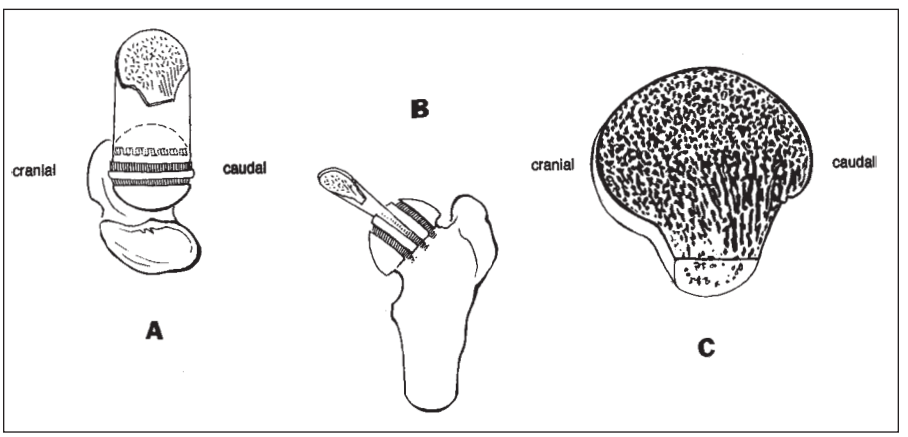

Figure 2—Illustration of transverse sectioning of the femoral head of a healthy dog. A—Proximal to distal view. B—Cranial to caudal view. C—Proximal to distal view of cancellous architecture.

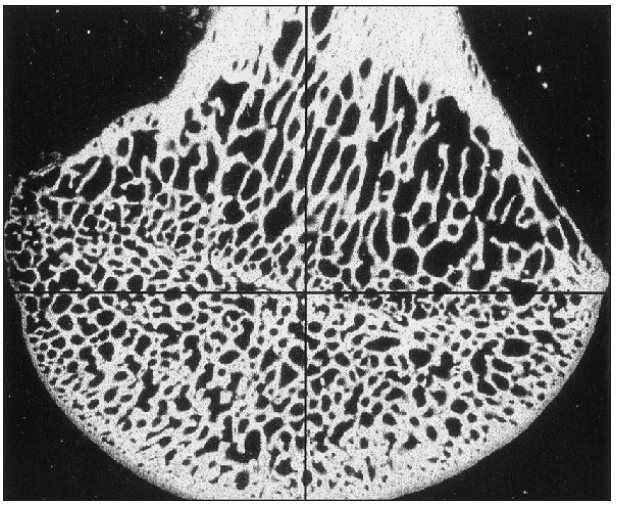

Figure 3—Computer image of coronal section of femoral head and neck of a healthy dog (articular surface is toward the bottom of the image; medial aspect of the femoral head is toward the left side of the image). Perpendicular lines are centered on the image to create 4 quadrants.

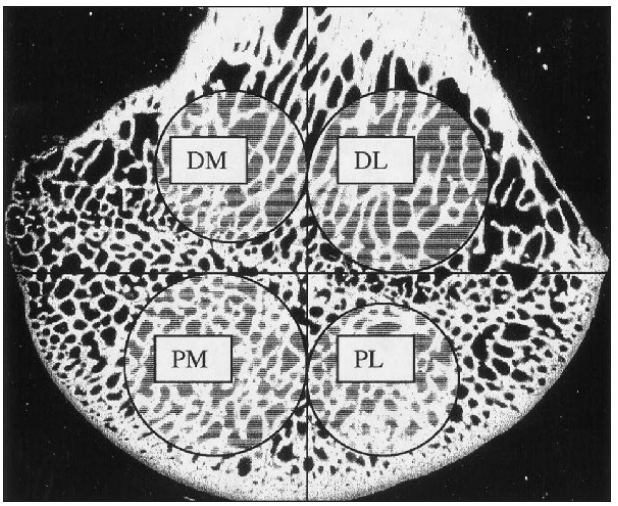

Figure 4—Computer image of coronal section of the femoral head and neck of a healthy dog, as in Figure 3. The 4 areas enclosed within circles are typical of regions selected for histomorphometric analysis. The largest possible circle that did not include the physeal scar or cortical bone was drawn in each quadrant. DM = Distomedial. DL = Distolateral. PL = Proximolateral. PM = Proximomedial.

microradiograph by use of a bone histomorphometry program.[1] Bone volume/total volume, trabecular thickness, and bone surface/total volume were recorded. The same area was outlined on the computer image, and the software was run at several potential threshold settings. Values for the same 3 parameters were recorded at each threshold setting. The threshold setting that resulted in the closest fit (bone volume ± 5%, trabecular thickness ± 30 µm, and bone surface ± 1.5 mm^2/mm^3) to hand-digitized values for all 4 computer images was selected for the software analysis of all images. All computer images were obtained from bone slices in an identical fashion, so we assumed the selected fixed threshold would calibrate the software for all images. Parallel line arrays and a grid made up of identical squares were analyzed by the software and produced predictable anisotropy data. Parallel lines resulted in anisotropy values of 100%, and the grid resulted in anisotropy values of < 1% (nearly isotropic, depending on where the analysis circle was placed on the grid).

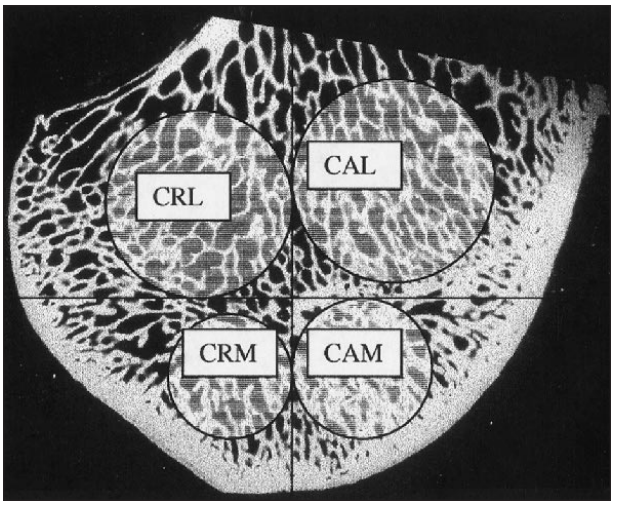

Figure 5—Computer image of a transverse section of the femoral head and neck of a healthy dog. The 4 areas enclosed within circles are typical of regions selected for histomorphometric analysis. The largest possible circle that did not include the physeal scar or cortical bone was drawn in each quadrant. CRL = Craniolateral. CAL = Caudolateral. CAM = Caudomedial. CRM = Craniomedial.

Four circular regions were selected for histomorphometric analysis in each bone section by 1 of the authors (DTE; **Fig 4 and 5**). A standard x-y axis was placed over the screen, centered on the image. The center of the x-y axis was placed at the estimated center of the physeal scar. If the scar was not evident, the axes were centered on the image. Two regions were encircled below the x axis (adjacent to the articular surface), and 2 regions were encircled above the x axis (distant from the articular surface) for each section. The largest fitting circle was encircled within each quadrant not crossing the physeal scar and not including subchondral plate or other cortical bone (Fig 4 and 5). Cortical bone was specifically excluded in our analysis to avoid confusing trabecular bone data with cortical bone data. Data recorded for each region were anisotropy, trabecular separation, bone volume/total volume, trabecular thickness, trabecular number, and bone surface/total volume. All histomorphometric indices were reported in accordance with the report of the American Society of Bone and Mineral Research for standardization.[23]

Cartilage—Sixteen femoral heads were collected from clinically normal dogs undergoing femoral head and neck excision in an unrelated study. Clinical evidence of coxofemoral discomfort or radiographic evidence of osteoarthritis were not detected. Macroscopic arthritic changes were not observed at surgery. Eight femoral heads were cut into 3 equal sections in the coronal plane, and 8 femoral heads were cut into 3 equal sections in the transverse plane. All sections were fixed in neutral-buffered 10% formalin and decalcified in citric-buffered formic acid. After paraffin embedding, 6-µm sections were obtained and stained with H & E and safranin O stains. Each section was divided into 4 equal segments, and the location of each segment on the femoral head was recorded. The sections were viewed under light microscopy and graded according to a revised Mankin method[20] (**Appendix**; a grade of 17 indicated healthy cartilage without defects) by 1 of the authors (PAM). The Mankin method uses systematic evaluation of the 4 zones of articular cartilage of adult dogs.[24] Twelve grades were generated for each femoral head (6 grades for each half of the femoral head).

Explanation of terms—Six parameters were evaluated: anisotropy (recorded as percentage orientation), **trabecular separation (TbSp**; µm), **bone volume (BV**; recorded as percentage of **total volume [TV**; BV/TV × 100]), **trabecular**

thickness (TbTh; μm), **mean trabecular number (TbN**; No./mm), and **bone surface area divided by total volume (BS/TV**; mm^2/mm^3).

Three variables were used to evaluate the relationships between parameters: slice location (cranial, middle, and caudal for the coronal plane, and dorsal, middle, and ventral for the transverse plane), division (proximal [adjacent to articular surface] and distal [distant from the articular surface] in the coronal sections; medial [adjacent to articular surface] and lateral [distant from the articular surface] in the transverse sections), and region (4 per section; **proximomedial [PM]**, **proximolateral [PL]**, **distomedial [DM]**, and **distolateral [DL]** for the coronal sections; **craniomedial [CRM]**, **caudomedial [CAM]**, **craniolateral [CRL]**, and **caudolateral [CAL]** for the transverse sections; Fig 4 and 5).

Coronal sectioning of the femoral head for cartilage analysis (into 3 equal sections) allowed division of the head into 6 lateral cartilage segments and 6 medial cartilage segments. Lateral and medial median cartilage grades were determined. Lateral and medial median cartilage grades corresponded to the PL and PM regions determined histomorphometrically. Transverse sectioning of the femoral head for cartilage analysis (into 3 equal sections) allowed division of the head into 6 cranial cartilage segments and 6 caudal segments. Cranial and caudal median cartilage grades were determined. The cranial and caudal median cartilage grades corresponded to the CRM and CAM regions determined histomorphometrically.

Statistical analyses—An ANOVA, using a split plot model, was used to evaluate the effect of slice location (cranial, middle, caudal for coronal sections; dorsal, middle, and ventral for transverse sections) and region on each parameter. One-way ANOVA was used to evaluate the effect of region (PM, PL, DL, and DM for the coronal orientation; CRL, CAL, CAM, and CRM for the transverse orientation) on each parameter. When results of ANOVA indicated significant differences within an orientation, a post hoc *t*-test was performed. Means of regions within each division were calculated, and the Student *t*-test was used to compare distal and proximal divisons for the coronal orientation, and lateral and medial divisions for the transverse orientation for each parameter. Cartilage data were considered nonparametric, and results were reported as median ± 95% confidence interval. Differences between cartilage halves (ie, medial vs lateral; cranial vs caudal) were evaluated by use of a Mann-Whitney U test. Variability within each region for bone histomorphometry and cartilage grading were determined (coefficient of variation = 100 × SD/mean). Differences were considered to be significant at $P < 0.05$.

Results

Bone—Forty-eight sections were prepared for image analysis. Two images (1 coronal and 1 transverse) were not analyzed because of inadequate contrast. In the coronally sectioned group, all significant differences among parameters were between regions that were in opposite divisions (**Table 1**). In other words, the 2 regions adjacent to the articular surface did not have significant differences among parameters, and the 2 regions distant from the articular surface did not have significant differences among parameters. In the transversely sectioned group, all significant differences among parameters were between regions that were in opposite divisions, with 1 exception; for anisotropy, a post hoc *t*-test identified significant differences between the craniolateral and caudolateral regions (**Table 2**).

Anisotropy was significantly greater in the distal and lateral divisions (femoral neck) than in the proximal and medial divisions (femoral head). Trabeculae were significantly more separated (larger TbSp) in the distal and lateral divisions than in the proximal and medial divisions. Bone volume and TbTh were significantly larger in the proximal and medial divisions than in the distal and lateral divisions. Trabecular number and BS/TV were significantly higher in the proximal and medial divisions than in the distal and lateral divisions.

Location of slice had a significant effect on anisotropy. In the coronal plane, anisotropy of the cranial slice was significantly ($P < 0.001$) greater than that of the middle and caudal slices. In the transverse plane, the anisotropy of the dorsal slice was significantly ($P < 0.001$) less than that of the middle and ventral slices.

Coefficients of variation of the histomorphometric parameters were lowest with TbN and BS/TV; values ranged from 9 to 18% and indicated high precision of the measurement. Trabecular thickness, BV, TbSp, and anisotropy had higher variation within regions, with values ranging from 23 to 60%.

Cartilage—Histologic grading of cartilage resulted in consistently high grades (healthy cartilage). Median cartilage grades from 8 dogs were determined for each half of cartilage to yield a single (median ± 95% confidence interval) grade. The medial half of cartilage that overlay PM region of cancellous bone had a grade of

Table 1—Histomorphometric indices (mean ± SD) of coronal sections of the proximal portion of the femur of healthy dogs

	Division			
	D		P	
Indices	**DM**	**DL**	**PM**	**PL**
Anisotropy (%)	28 ± 11	22 ± 13	12 ± 5	14 ± 6
TbSp (mm)	349 ± 125	370 ± 110	253 ± 75	267 ± 88
BV/TV (%)	32 ± 13	28 ± 11	44 ± 16	43 ± 16
TbTh (mm)	156 ± 59	140 ± 50	198 ± 76	200 ± 83
TbN (mm^{-1})	2.59 ± 0.39	2.57 ± 0.44	2.85 ± 0.29	2.78 ± 0.38
BS/TV (mm^2/mm^3)	5.2 ± 0.8	5.1 ± 0.9	5.7 ± 0.6	5.6 ± 0.8

D = Regions distal to the physeal scar. P = Regions proximal to the physeal scar. DM = Distomedial. DL = Distolateral. PM = Proximomedial. PL = Proximolateral. Anisotropy = Trabecular alignment. TbSp = Trabecular separation. BV/TV = Bone volume/total volume. TbTh = Trabecular thickness. TbN = Trabecular number. BS/TV = Bone surface/total volume.

Differences between all D and P values were significant ($P < 0.005$).

Table 2—Histomorphometric indices (mean ± SD) of transverse sections of the proximal portion of the femur of healthy dogs

	Division			
	L		M	
Indices	**CRL**	**CAL**	**CAM**	**CRM**
Anisotropy (%)	14 ± 6	30 ± 7*	16 ± 8	14 ± 6
TbSp (mm)	430 ± 150	432 ± 175	295 ± 77	299 ± 89
BV/TV (%)	29 ± 10	28 ± 11	44 ± 11	43 ± 13
TbTh (mm)	163 ± 49	151 ± 53	231 ± 61	226 ± 71
TbN (mm^{-1})	2.20 ± 0.30	2.26 ± 0.36	2.44 ± 0.23	2.44 ± 0.23
BS/TV (mm^2/mm^3)	4.4 ± 0.6	4.5 ± 0.7	4.9 ± 0.5	4.9 ± 0.5

*Significant ($P < 0.001$) difference between CAL and CRL.

L = Regions lateral to the physeal scar. M = Regions medial to the physeal scar. CRL = Craniolateral. CAL = Caudolateral. CAM = Caudomedial. CRM = Craniomedial.

Differences between all L and M values were significant ($P < 0.001$).

See Table 1 for remainder of key.

16.2 ± 0.4 with a coefficient of variation of 3%. The lateral half of cartilage that overlay the PL region of cancellous bone had a grade of 15.9 ± 0.6 with a coefficient of variation of 5%. The cranial half of cartilage that overlay the CRM region of cancellous bone had a grade of 16.6 ± 0.2 with a coefficient of variation of 2%. The caudal half of cartilage that overlay the CAM region of cancellous bone had a grade of 16.3 ± 0.3 with a coefficient of variation of 3%.

Discussion

Results of the study reported here provide morphometric quantification of the cancellous bone of the proximal portion of the femur of healthy dogs. Because trabecular alignment was higher in the femoral neck than in the femoral head when viewed from 2 planes that were perpendicular to each other, we could extrapolate an image of rod-shaped trabeculae aligned parallel to the long axis of the femoral neck (Fig 1C). These aligned trabeculae in the neck the randomly arranged trabeculae in the femoral head at the physeal scar. The caudal part of the neck had significantly higher anisotropy than the cranial part (Fig 2C), suggesting that the aligned trabeculae of the femoral neck were confined to the caudal half of the neck. The cranial part of the neck had trabeculae that were more isotropically or randomly arranged and were not significantly different from the pattern in the femoral head (Fig 2C).

The Singh et al[5] description of 5 distinct, trabecular groupings in the proximal portion of the femur in humans is based on each trabecular group acting to oppose compressive or tensile forces. In healthy humans, trabeculae in the upper end of the femur are arranged along the lines of compression and tension stresses produced in the bone during weight bearing.[5] Results of our study indicate that the caudal part of the femoral neck in healthy dogs has a grouping of aligned trabeculae. We cannot state whether this trabecular group opposes compressive or tensile forces, but we can make some load distribution assumptions on the basis of trabecular orientation.[4,5,25] The femoral head of dogs, with its random trabecular arrangement, distributes a load from many directions, whereas the neck receives a more consistent load caudally. Our finding of 1 distinct trabecular grouping (in contrast with 5 trabecular groupings) is perhaps the result of different loading of the hip joint in quadrupedal animals such as dogs, compared with that of bipedal humans.[26,27]

Cartilage grades were determined from different femoral heads than those used for histomorphometric analysis. This was unavoidable because of collection methods, the need for different types of histologic processing for each analysis, and the size of the femoral heads. Nevertheless, histomorphometry and cartilage grading were determined from femurs harvested from clinically normal dogs that did not have radiographic or macroscopic evidence of osteoarthritis. The minimal variation in cartilage data (2 to 5 %) assured us that we had sampled a nonarthritic population, although subtle, early osteoarthritic changes may be missed by the revised Mankin grading method.

Significant differences were not detected among histomorphometric parameters in bone regions (PM, PL, CRM, CAM) adjacent to the articular surface. Variability, however, was much higher in the bone analysis data than in the cartilage data. Higher variability in the bone data suggested that there is a large amount of variation among nonarthritic dogs, or, perhaps, that our selection of dogs included those with a certain degree of pathologic cancellous remodeling. Our criteria for including dogs in the bone analysis were identical to those for the cartilage analysis, and low variability in the cartilage data supports our contention that these dogs were also healthy and nonarthritic. We concluded that healthy articular cartilage of the femoral head of dogs had underlying cancellous bone with a typical range of values for anisotropy, TbSp, BV/TV, TbTn, TbN, and BS/TV.

Two-dimensional histomorphometry that used` the method of directed secants was accessible and rapid for our purpose of describing the cancellous architecture of large sections (2 to 3 cm wide) of bone. Two-dimensional stereology has been used as the standard method to assess the accuracy of three-dimensional systems such as **micro-computed tomography (micro CT)** or magnetic resonance imaging.[22,28-30] Three-dimensional descriptions of cancellous architecture are appealing in their depiction of trabecular interconnections,[22,28-30] and histomorphometric indices and anisotropy may be better quantified in 3 dimensions.[31] Kuhn et al[30] compared two-dimensional morphometric data with micro CT. Mean stereologic measurements of bone volume fraction, mean trabecular plate thickness, mean trabecular plate density, and mean trabecular plate separation were computed by use of 5 consecutive, 10-µm-thick histologic sections. Results were compared with calculations from a 50-µm-thick, micro CT slice of the same bone region. Kuhn et al[30] concluded that micro CT results compared favorably with the accepted two-dimensional data, but resolution was limited (> 50 µm/pixel on cubes of bone > 8 mm wide).[30] Although two-dimensional imaging does not allow description of trabecular shape and interconnection in a third plane, we used perpendicular sectioning planes to estimate the trabecular architecture in 3 dimensions.

Limitations in creating accurate representations of the trabecular bone for computer analysis influenced our results. Sawing, grinding, making microradiographs, scanning, thresholding, and selection of analysis regions created many areas of influence on the data. Distortion of trabecular architecture may be avoided by capturing high-detail photographic images of a section prior to cutting it from the parent bone.[30,31] Direct photographic images would bypass the radiographic step, which may blur the distinction between bone and air and result in contrast that varies with thickness of samples. Some of the variability in the histomorphometric results may have been eliminated by photographing or even directly scanning the cut surface of the parent bone. In addition, if the femoral head and neck had been further segregated into smaller regions for analysis, additional groupings of aligned trabeculae may have been noticed. We were concerned, however, that locating the same small regions from 1 computer image to the next would be difficult.

Software that uses the method of directed secants allows rapid, accurate analysis of trabecular bone[16,21,22,29] but is dependent on the creation of a binary image with

a thresholding technique. A fixed threshold, as was used in this study, causes problems with geometric and density variations in the images. Kuhn et al[30] wrote that "the actual borders of each trabeculae exist somewhere within the transition regions between the low density of marrow or air, and the high density corresponding to the center of the trabecula." It is possible to make thick trabeculae even thicker and thin trabeculae disappear with a fixed threshold. Less mineralized bone could also be inaccurately imaged. Several of the computer images in our study were analyzed throughout a range of fixed thresholds, and we compared the same sections by analysis with a commercially available histomorphometry program that used hand digitizing. Although we think the selected threshold created binary images that were true to the original bone architecture, subjectivity in the hand-digitizing (tracing bone edges from the microradiographs) and contrast variations amongst the microradiographs may have caused some loss of accuracy.

[a]Model 11-2480 Isomet, Buehler Ltd, Lake Bluff, Ill.
[b]Polysciences Inc, Warrington, Penn.
[c]Model ML521D, Hacker Instruments Inc, Fairfield, NJ.
[d]Industrex SR High resolution film, Eastman Kodak Co, Rochester, NY.
[e]Model 43855A, Faxitron, Hewlett-Packard, McMinnville, Ore.
[f]45 LeafScan 2.2scsi, LeafSystems Inc, Southboro, Mass.
[g]7100/80 Power Macintosh System 7.6, Apple Computer Inc, Cupertino, Calif.
[h]Adobe Photoshop Version 3.0.3, Adobe Systems Inc, San Jose, Calif.
[i]OsteoMeasure, Version 2.2, Osteometrics Inc, Atlanta, Ga.

Appendix

Histologic-histochemical grading system for articular cartilage

Grade	Cartilage structure
6	No abnormalities
5	Surface irregularities
4	Pannus and surface irregularities
3	Clefts from surface to transitional zone and superficial disorganization; loss of boundary between tangential and transitional zones
2	Clefts from surface to radiate zone with or without disorganization of radiate zone and with or without loss of superficial layer(s)
1	Progression of cartilage loss into radiate zone; with or without clefts to radiate zone or the calcified zone
0	Cartilage eroded down to the calcified zone (eburnation)
Grade	**Cells**
4	Typical number
3	Diffuse hypercellularity
2	Cloning
1	Hypocellularity
0	Severe hypocellularity and cartilage loss
Grade	**Staining**
5	Typical
4	Slight reduction in staining with or without staining reduced in radiate zone
3	Moderate reduction in staining with or without reduction in interterritorial matrix
2	Staining only in pericellular matrix
1	Staining absent with or without occasional rim of pericellular matrix staining
0	Staining absent and severe cartilage loss
Grade	**Calcified zone integrity**
2	Intact
1	Crossed by blood vessels
0	Tidemark absent, severe cartilage loss

References

1. Meyer GH. Die Architektur der Spongiosa. *Arch Anat Physiol wiss Med* 1867;34:615–628.
2. Wolff J. Über die innere Architektur der Knochen unde ihre Bedeutung für die Frage vom Knochenwachstum. *Virchows Arch Pathol Anat Physiol* 1870;50:389–453.
3. Garden RS. The structure and function of the proximal end of the femur. *J Bone Joint Surg [Br]* 1961;43:576–589.
4. Pauwels F. On the distribution of the density of cancellous bone in the upper end of the femur and its significance for the theory of the functional structure of bone. In: *Biomechanics of the locomotor apparatus: contributions on the functional anatomy of the locomotor apparatus*. New York: Springer-Verlag Inc, 1980;299–309.
5. Singh B, Nagrath AR, Maini PS. Changes in trabecular pattern of the upper end of the femur as an index of osteoporosis. *J Bone Joint Surg [Am]* 1970;52:457–467.
6. Whitehouse WJ, Dyson ED. Scanning electron microscope studies of trabecular bone in the proximal end of the human femur. *J Anat* 1974;118:417–444.
7. Elke RPE, Cheal EJ, Simmons C, et al. Three-dimensional anatomy of the cancellous structures of the human proximal femur from computed tomography data. *J Orthop Res* 1995;13:513–523.
8. Goldstein SA. The mechanical properties of trabecular bone: dependence on anatomic location and function. *J Biomech* 1987;20:1055–1061.
9. Roesler H. The history of some fundamental concepts in bone biomechanics. *J Biomech* 1987;20:1025–1034.
10. Vahey JW, Lewis JL, Vanderby R Jr. Elastic moduli, yield stress, and ultimate stress of cancellous bone in the canine proximal femur. *J Biomech* 1987;20:29–33.
11. Radin EL, Paul IL, Lowy M. A comparison of the dynamic force transmitting properties of subchondral bone and articular cartilage. *J Bone Joint Surg [Am]* 1970;52:444–456.
12. Radin EL, Rose RM. Role of subchondral bone in the initiation and progression of cartilage damage. *Clin Orthop* 1986;213:34–40.
13. Radin EL, Parker HG, Pugh JW, et al. Response of joints to impact loading—III: relationship between trabecular microfractures and cartilage degeneration. *J Biomech* 1973;6:51–57.
14. Radin EL, Orr RB, Kelman JL, et al. Effect of prolonged walking on concrete on the knees of sheep. *J Biomech* 1982;15:487–492.
15. Pugh JW, Radin EL, Rose RM. Quantitative studies of human subchondral cancellous bone: its relationship to the state of its overlying cartilage. *J Bone Joint Surg [Am]* 1974;56:313–321.
16. Hayes WC, Snyder B. Toward a quantitative formulation of Wolff's law in trabecular bone. In: Cowen SC, ed. *Mechanical properties of bone*. New York: ASME, 1981;43–68.
17. Pugh JW, Rose RM, Radin EL. Elastic and viscoelastic properties of trabecular bone: dependence on structure. *J Biomech* 1973;6:475–485.
18. Fyhrie DP, Carter DR. A unifying principle relating stress to trabecular bone morphology. *J Orthop Res* 1986;4:304–317.
19. Pugh JW, Rose RM, Radin EL. A structural model for the mechanical behavior of trabecular bone. *J Biomech* 1973;6:657–670.
20. Mankin MJ, Lippiello L, Zarins A. Biochemical and metabolic abnormalities in articular cartilage from osteo-arthritic human hips. II. Correlation of morphology with biochemical and metabolic data. *J Bone Joint Surg [Am]* 1971;53:523–537.
21. Whitehouse WJ. The quantitative morphology of anisotropic trabecular bone. *J Microscopy* 1974;101:153–168.
22. Hipp JA, Jansujwicz A, Simmons CA, et al. Trabecular bone morphology from micro-magnetic resonance imaging. *J Bone Miner Res* 1996;11:286–292.
23. Parfitt AM, Drezner MK, Glorieux FH, et al. Bone histomorphometry: standardization of nomenclature, symbols, and units. *J Bone Miner Res* 1987;2:595–609.
24. Rodkey WG, McKinney LA. Review of structure, function, and composition of cartilage and synovium. In: Bojrab MJ, Smeak DD, Bloomberg MS, eds. *Disease mechanisms in small animal surgery*. Philadelphia: Lea & Febiger, 1993;649–655.
25. Vander Sloten J, Van der Perre G. Trabecular structure compared to stress trajectories in the proximal femur and the calcaneus. *J Biomed Eng* 1989;11:203–208.
26. Hildebrand, M. Mechanics of support and movement. In:

Analysis of vertebrate structure. New York: John Wiley & Sons, 1982;411–462.

27. Jenkins FA Jr, Camazine SM. Hip structure and locomotion in ambulatory and cursorial carnivores. *J Zool [Br]* 1977;181:351–370.

28. Feldkamp LA, Goldstein SA, Parfitt AM, et al. The direct examination of three-dimensional architecture in vitro by computed tomography. *J Bone Miner Res* 1989;4:3–11.

29. Muller R, Hahn M, Vogel M, et al. Morphometric analysis of noninvasively assessed bone biopsies: comparison of high-resolution computed tomography and histologic sections. *Bone* 1996;18:215–220.

30. Kuhn JL, Goldstein SA, Feldkamp LA, et al. Evaluation of a microcomputed tomography system to study trabecular bone structure. *J Orthop Res* 1990;8:833–842.

31. Odgaard A, Andersen K, Melsen F, et al. A direct method for fast three-dimensional serial reconstruction. *J Microscopy* 1990;159: 335–342.